Neuro-Oncology

Neuro-Oncology 18(12), 1610–1621, 2016
doi:10.1093/neuonc/now112
Advance Access date 10 June 2016

Limited role for transforming growth factor–β pathway activation-mediated escape from VEGF inhibition in murine glioma models

Davide Mangani, Michael Weller, Emad Seyed Sadr, Edith Willscher, Katharina Seystahl, Guido Reifenberger, Ghazaleh Tabatabai†, Hans Binder, and Hannah Schneider

Laboratory of Molecular Neuro-Oncology, Department of Neurology, University Hospital and University of Zurich, Zurich, Switzerland (D.M., M.W., E.S.S., K.S., G.T., H.S.); Center for Neuroscience, University of Zurich, Zurich, Switzerland (M.W., G.T.); Interdisciplinary Center for Bioinformatics, University of Leipzig, Leipzig, Germany (E.W., H.B.); Institute of Neuropathology, Heinrich Heine University, Düsseldorf, Germany (G.R.); German Cancer Consortium (DKTK), German Cancer Research Center (DKFZ) Heidelberg, partner site, Essen/Düsseldorf, Germany (G.R.)

Corresponding Author: Michael Weller, MD, Department of Neurology, University Hospital Zurich, Zurich, Switzerland (michael.weller@usz.ch).

†Current address: Interdisciplinary Division of Neuro-Oncology, University Hospital Tuebingen, Laboratory of Clinical and Experimental Neuro-Oncology, Hertie Institute for Clinical Brain Research, Eberhard Karls University, Tuebingen, Germany.

Background. The vascular endothelial growth factor (VEGF) and transforming growth factor (TGF)–β pathways regulate key biological features of glioblastoma. Here we explore whether the TGF-β pathway, which promotes angiogenesis, invasiveness, and immunosuppression, acts as an escape pathway from VEGF inhibition.

Methods. The role of the TGF-β pathway in escape from VEGF inhibition was assessed in vitro and in vivo and by gene expression profiling in syngeneic mouse glioma models.

Results. We found that TGF-β is an upstream regulator of VEGF, whereas VEGF pathway activity does not alter the TGF-β pathway in vitro. In vivo, single-agent activity was observed for the VEGF antibody B20-4.1.1 in 3 and for the TGF-β receptor 1 antagonist LY2157299 in 2 of 4 models. Reduction of tumor volume and blood vessel density, but not induction of hypoxia, correlated with benefit from B20-4.1.1. Reduction of phosphorylated (p)SMAD2 by LY2157299 was seen in all models but did not predict survival. Resistance to B20 was associated with anti-angiogenesis escape pathway gene expression, whereas resistance to LY2157299 was associated with different immune response gene signatures in SMA-497 and GL-261 on transcriptomic profiling. The combination of B20 with LY2157299 was ineffective in SMA-497 but provided prolongation of survival in GL-261, associated with early suppression of pSMAD2 in tumor and host immune cells, prolonged suppression of angiogenesis, and delayed accumulation of tumor infiltrating microglia/macrophages.

Conclusions. Our study highlights the biological heterogeneity of murine glioma models and illustrates that cotargeting of the VEGF and TGF-β pathways might lead to improved tumor control only in subsets of glioblastoma.

Keywords: coinhibition, escape mechanism, glioblastoma, TGF-β, VEGF.

Glioblastoma remains a universally fatal neoplasm despite some advances in its multidisciplinary management—for instance, the introduction of combined modality treatment, including postsurgical radiotherapy (RT) with concomitant and maintenance temozolomide (TMZ/RT→TMZ).[1,2] Several current strategies of glioblastoma treatment focus on the inhibition of angiogenesis, largely the vascular endothelial growth factor (VEGF) pathway. Yet, the lead compound bevacizumab has not been approved in Europe for treatment of recurrent glioblastoma because an effect on overall survival has not been demonstrated, and the recently completed EORTC 26101 trial failed to demonstrate superior survival with the combination of bevacizumab with lomustine over lomustine alone.[3] Further, 2 phase III trials in the newly diagnosed setting achieved prolonged progression-free survival but not overall survival.[4,5] While the potential clinical benefit of improving progression-free survival is not disputed, these study results call for combination therapies of VEGF antagonism with other targeted agents that may extend progression-free survival further and confer a survival benefit.

One likely explanation for the failure of VEGF antagonism to prolong overall survival is the induction of a biological change in tumors that eventually fail bevacizumab and then seem to be

Received 16 February 2016; accepted 22 April 2016

rather refractory to all further treatments. While it has been claimed that VEGF antagonism induces a more infiltrative phenotype in animal models,[6] this assumption has been confirmed neither in retrospective analyses of recurrent glioblastoma patients[7] nor in the AVAglio trial.[8]

Transforming growth factor (TGF)-β is a multifunctional cytokine implicated in the pathogenesis of glioblastoma, based on immunosuppressive properties and promotion of migration, invasion, angiogenesis, and stem cell maintenance.[9] Therapeutic activity of TGF-β antagonism has been demonstrated in animal models of glioma, but translation of TGF-β antagonism into the clinic has remained challenging. The most advanced TGF-β antagonist is the receptor kinase inhibitor LY2157299,[10,11] which is currently being explored in newly diagnosed and recurrent glioblastoma. There are multiple potential interdependencies between angiogenesis and the TGF-β pathway. Importantly, TGF-β has been identified as a positive upstream regulator of VEGF mRNA expression and release and angiogenesis in cancer and nonneoplastic cells,[12–16] providing a strong rationale for combining TGF-β and VEGF inhibition. Accordingly, we here explored the crosstalk between these pathways in syngeneic murine glioma models and asked whether cotargeting the VEGF and TGF-β pathways provides a new perspective for the treatment of glioblastoma.

Materials and Methods

Reagents

Recombinant human TGF-β_2 was purchased from R&D Systems and murine VEGF ($VEGF_{120}$) from Biolegend. B20-4.1.1 (B20) was kindly provided by T. R. Schwartz (Genentech), cediranib by AstraZeneca, and LY2157299 (LY) by Eli Lilly.

Cell Lines

Murine SMA-497, SMA-540, and SMA-560 glioma cells were kindly provided by D. D. Bigner. GL-261 cells were received from the National Cancer Institute.

Viability and Clonogenicity Assays

Viability was assessed after pooling adherent and floating cells by trypan blue dye exclusion. Clonogenicity was assessed as previously described.[17] Cells were treated with either 1 μM LY2157299, 100 nM cediranib, or 100 μg/mL B20.

Real-time PCR

Total mRNA for gene expression analyses was extracted from murine glioma cells after 24 h incubation in serum-free medium or from in vivo tumor tissue.[13] For real-time PCR, gene expression was measured using the Real Time PCR System 7300 (Applied Biosystems) with SYBR Green Master Mix (AppliChem) and primers at optimized concentrations.

Immunoblot Analyses

For immunoblot analysis, whole cell lysates were prepared and proteins were separated under denaturating conditions following blotting and antibody detection.

Enzyme-linked Immunosorbent Assay

Supernatants from subconfluent glioma cell cultures (treated or untreated) were analyzed.

Animal Studies

The care and treatment of all animals was in accordance with the Swiss Federal Law on the Protection of Animals, the Swiss Federal Ordinance on the Protection of Animals, and the guidelines of the Swiss confederation (permission #38/2012). For intracranial tumor cell implantation, 2 μL of a single cell suspension in phosphate buffered saline was injected (1 μL/min) into the right striatum. Five thousand cells of SMA or 20 000 cells of GL-261 were implanted in VM/Dk or C57BL/6 mice, respectively ($n = 10$ per group).

Immunohistochemical Analysis

Cryosections were fixed, blocked, and stained with primary, followed by secondary, antibodies. Subsequently, quantification of immunohistological staining was performed.

Immunofluorescence Microscopy

Immunofluorescence studies were carried out on cryosections of tumor-bearing mouse brains, and data analysis was performed with Bitplane Imaris software.[18]

Analysis of Gene Expression Data

The generation of the microarray analyzed herein has been described.[19]

Statistical Analyses

All in vitro data are representative of experiments performed in 3 independent experiments with similar results. All statistical analyses were performed using GraphPad Prism 5. For additional methods, please see the Supplementary material.

Results

Characterization of VEGF and TGF-$\beta_{1/2}$ Ligand/Receptor Expression in Mouse Glioma Cells

VEGF-A (*VEGF*) mRNA was constitutively expressed by all cell lines, with the highest levels in GL-261 and SMA-560. In contrast, the highest levels of protein release were observed in SMA-540 and SMA-560 (Fig. 1A). VEGF receptor (*VEGFR*)1 mRNA was expressed in all cell lines, and protein levels correlated well, with highest levels in SMA-560. SMA-560 showed the highest *VEGFR2* mRNA levels, followed by SMA-540, and protein was detected in only SMA-540 and SMA-560 (Fig. 1B). We also examined ex vivo tumoral mRNA expression of ligands and receptors, using syngeneic normal brain tissue of VM/Dk and C57BL/6 mice as a reference. In vitro maintained monolayer cultures (MC) and mouse gliomas in vivo (T) showed similar *VEGF* mRNA levels (Supplementary Fig. S1A). Compared with MC, there were higher *VEGFR1* mRNA in SMA-497 and GL-261, and higher *VEGFR2* mRNA levels in all models in vivo (Supplementary Fig. S1B and C), suggesting a major

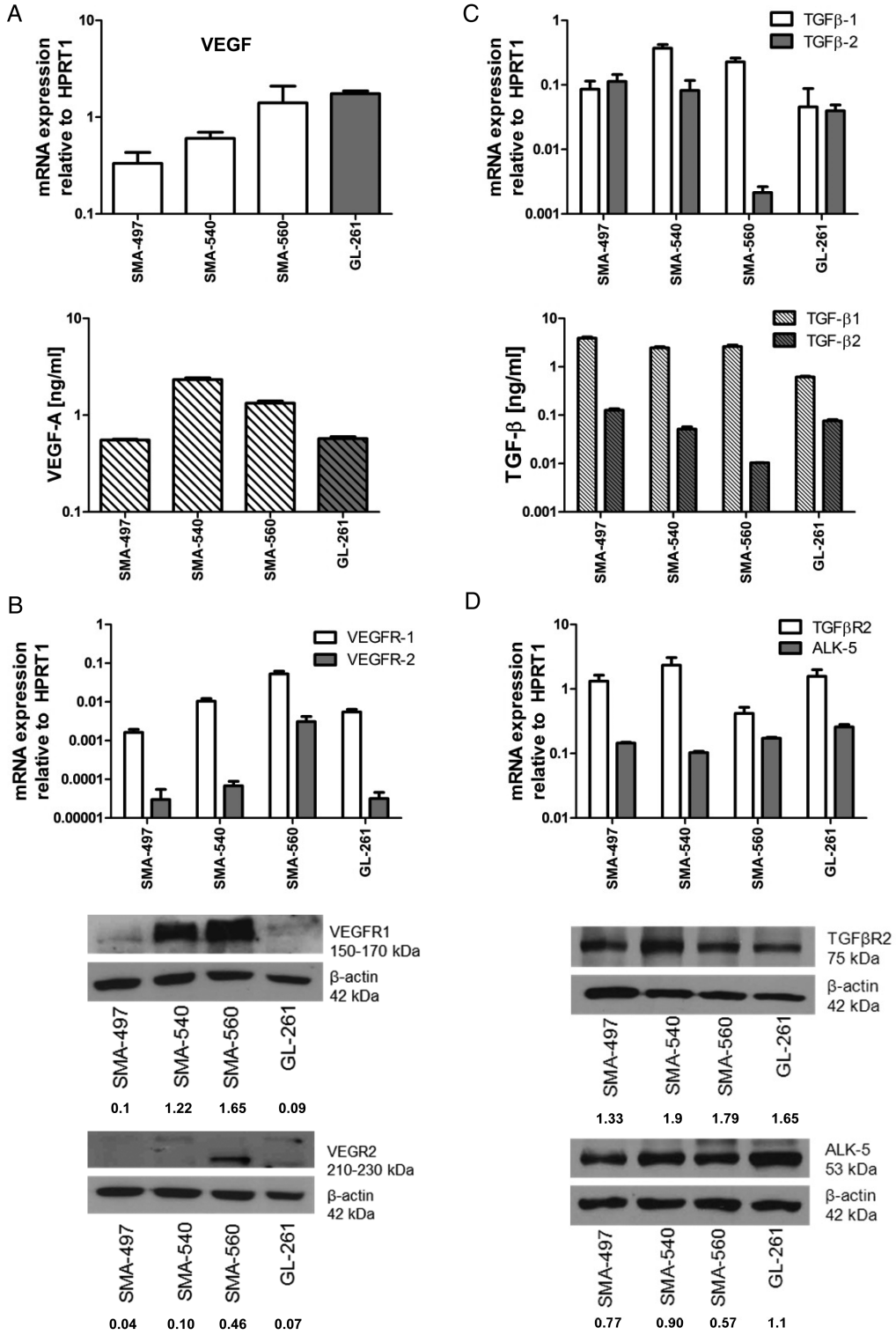

Fig. 1. Expression of VEGF and TGF-β pathway ligands and receptors in mouse glioma models in vitro. SMA-497, SMA-540, SMA-560, and GL-261 cells were studied for gene expression. (A) VEGF expression determined by real-time (RT)-PCR for mRNA (top) and by enzyme-linked immunosorbent assay (ELISA) for protein in the supernatant (bottom) in vitro. (B) VEGFR1/2 expression determined by RT-PCR (top) and immunoblot (bottom) in vitro. (C) TGF-β1/2 expression determined by RT-PCR (top) and ELISA in the supernatant (bottom) in vitro. (D) TGF-βR2 and ALK-5 expression determined by RT-PCR (top) and immunoblot (bottom) in vitro. Values of densitometric analysis relative to β-actin are shown below the immunoblot panels in (B) and (D). HPRT1, hypoxanthine phosphoribosyltransferase 1.

contribution from tumor blood vessels or upregulation of expression in tumor cells in vivo. Immunohistochemical stainings of VEGFR2 levels revealed a major contribution from tumor cells, even masking a typical vessel staining pattern, which, however, became readily visible in tumors stained for CD31 (see below) (Supplementary Fig. S1D and E).

TGFβ$_{1/2}$ mRNA was abundant in all 4 models. There was no apparent correlation between mRNA and protein levels, and TGF-β_1 consistently exceeded TGF-β_2 protein levels in the supernatant. TGF-β receptor 2 (TGFβR2) and activin receptor-like kinase 5 (*ALK-5*) were expressed in all models at variable levels, with correlation between mRNA and protein (Fig. 1C and D). *TGFβ*$_1$ but not *TGFβ*$_2$ mRNA was enhanced in vivo in SMA-497, SMA-560, and GL-261. While *ALK5* mRNA was consistently increased in vivo, there was a mixed pattern for *TGFβR2* mRNA expression with increased expression in SMA-560, and a trend

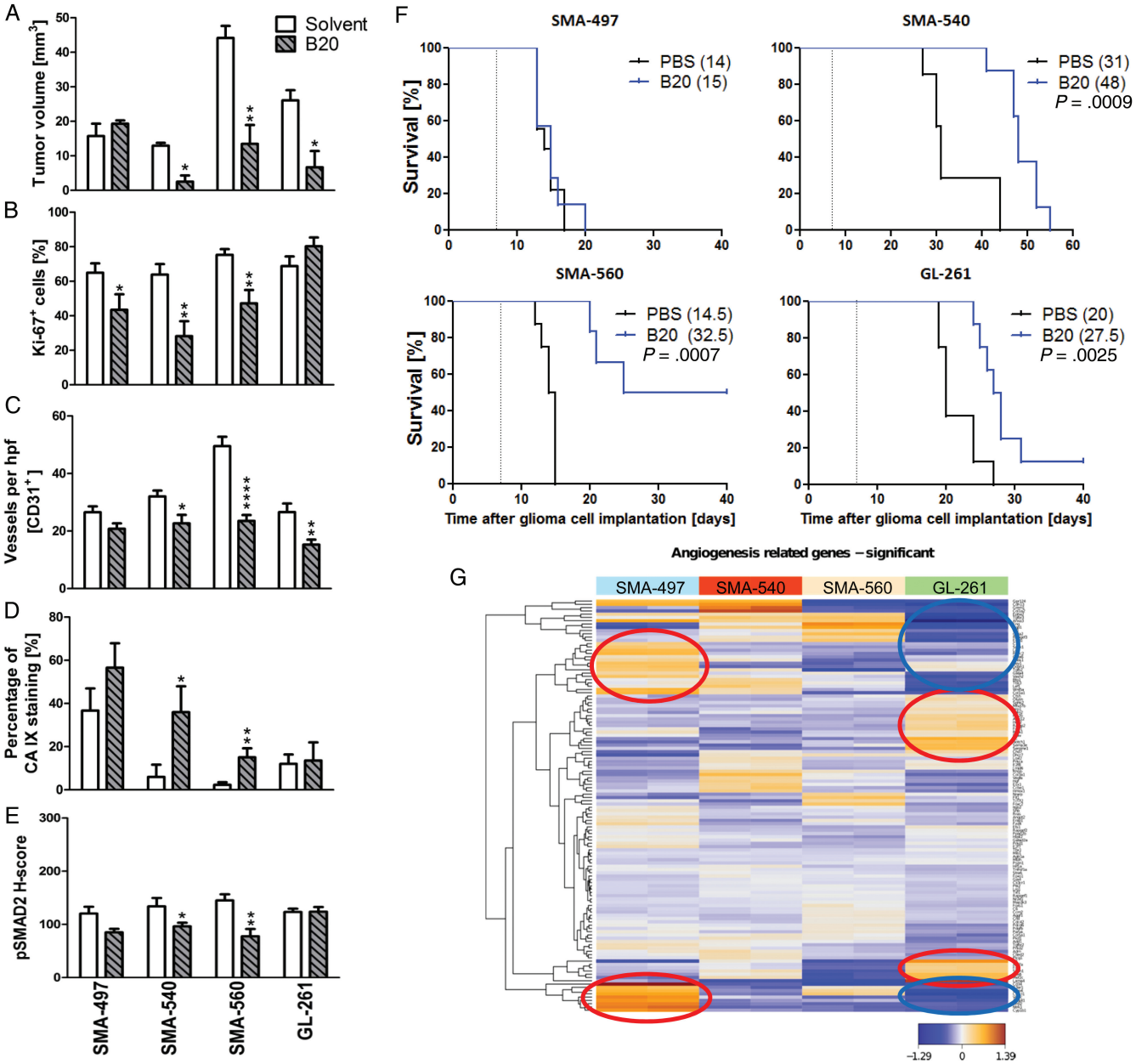

Fig. 2. Differential effects of murinized bevacizumab on angiogenesis and growth of murine gliomas. Syngeneic mice intracranially implanted with SMA-497, SMA-540, SMA-560, or GL-261 cells were treated twice weekly with 5 mg/kg B20 or phosphate buffered saline from day 7 on. Brain sections (early-stage) were analyzed. (A) Tumor volumes. (B) Ki-67. (C) CD31+ capillaries. (D) CA 9+ areas. (E) pSMAD2. Data are expressed as mean + SEM (*$P < .05$, **$P < .01$, ****$P < .0001$, unpaired Student's *t*-test, B20 vs solvent). (F) Kaplan–Meier survival curves of glioma-bearing mice (log-rank test, considered significant for $P < .05$). (G) Angiogenic gene expression heatmaps obtained by unsupervised comparison of genes differentially expressed in the 4 mouse glioma cell lines. The heatmaps indicate high to low expression levels as red to blue color coding. Up- or downregulated gene clusters in SMA-497 and GL-261 cells are encircled in red or blue.

for decreased expression in the other models (Supplementary Fig. S1F–I).

Modulation and Consequences of VEGF and TGF-$\beta_{1/2}$ Signaling In vitro

We observed an increase in phosphorylated (p)VEGFR1 levels in response to exogenous VEGF in SMA but not in GL-261 glioma cells. Phosphorylated VEGFR2 was increased upon VEGF stimulation in SMA-540 and SMA-560 (Supplementary Fig. S2A). An increase in pSMAD2 was observed in all models after exposure to exogenous TGF-β_2. LY2157299 attenuated constitutive and induced SMAD2 phosphorylation (Supplementary Fig. S2B). Neither VEGF pathway inhibition using B20 nor relevant concentrations of cediranib nor TGF-β pathway inhibition by LY2157299 affected viability or clonogenicity (Supplementary Fig. S2D and E).

Murinized Bevacizumab Prolongs Survival in SMA-540, SMA-560, and GL-261 Glioma Models

We next determined single-agent activity of B20 treatment in the 4 mouse glioma models. Histological analyses of tumors harvested when the first clinical symptoms occurred (early-stage) revealed reduced tumor volumes in all models except SMA-497. Tumor volume reduction was not paralleled by changes in Ki-67 labeling (Fig. 2A and B). Solvent-treated

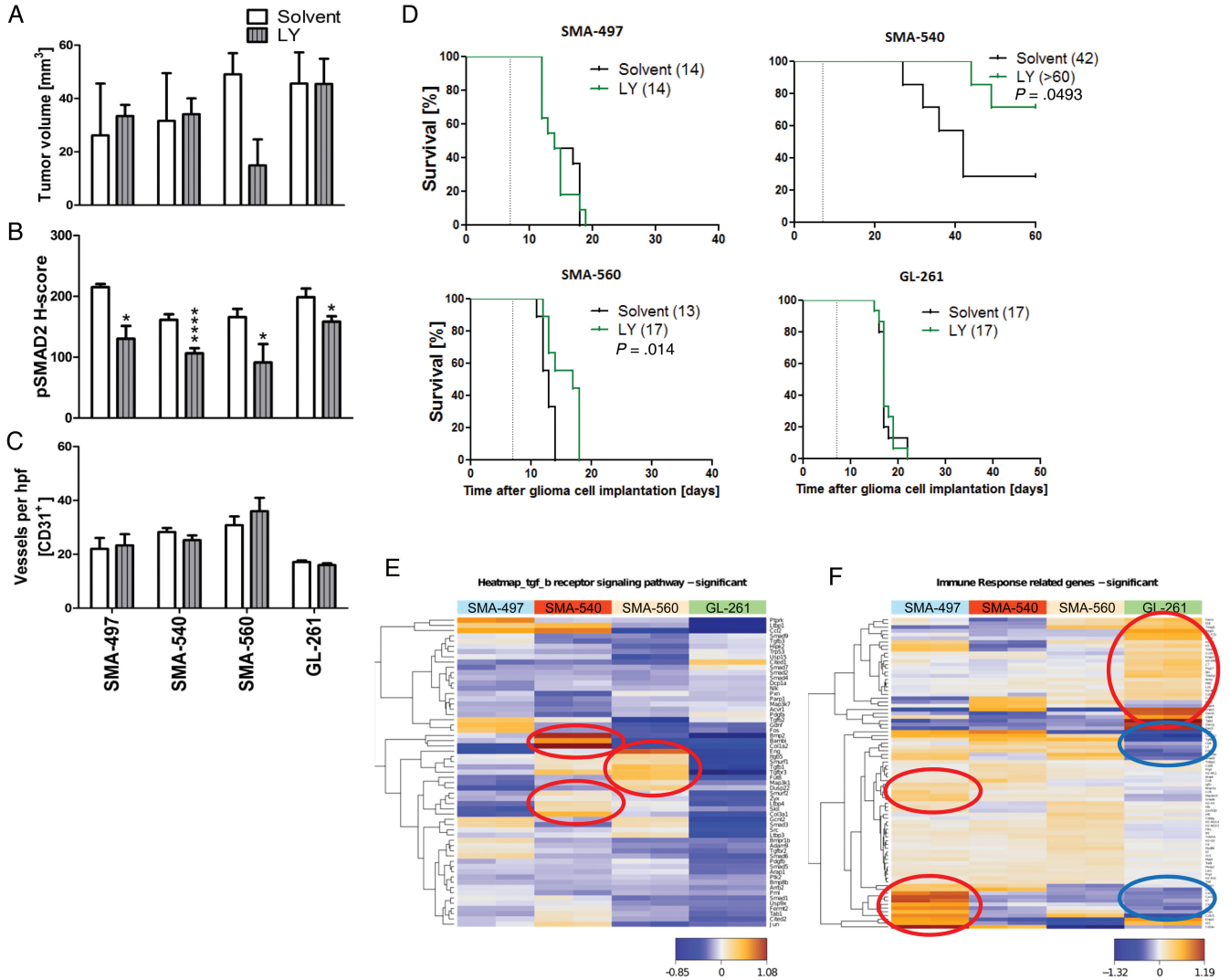

Fig. 3. Differential effects of LY2157299 on the growth of murine gliomas. Mice intracranially implanted with SMA-497, SMA-540, SMA-560, or GL-261 cells were treated daily with LY2157299 at 150 mg/kg or control solvent from day 7 on. Brain sections (early-stage) were analyzed. (A) Tumor volumes. (B) pSMAD2 and CD31+ capillaries. (C) Data are expressed as mean + SEM (*$P < .05$, ****$P < .0001$, unpaired Student's *t*-test, LY2157299 vs solvent). (D) Kaplan–Meier survival curves of glioma-bearing mice (log-rank test was considered significant for $P < .05$). (E, F) Gene expression heatmaps were obtained by unsupervised comparison of genes differentially expressed in the 4 mouse glioma cell lines for the TGF-β signaling (E) and immune response (F) pathways. The heatmaps indicate high to low expression levels as red to blue color coding. Up- or downregulated gene clusters in SMA-497 and GL-261 cells are encircled in red or blue. hpf, high-powered field.

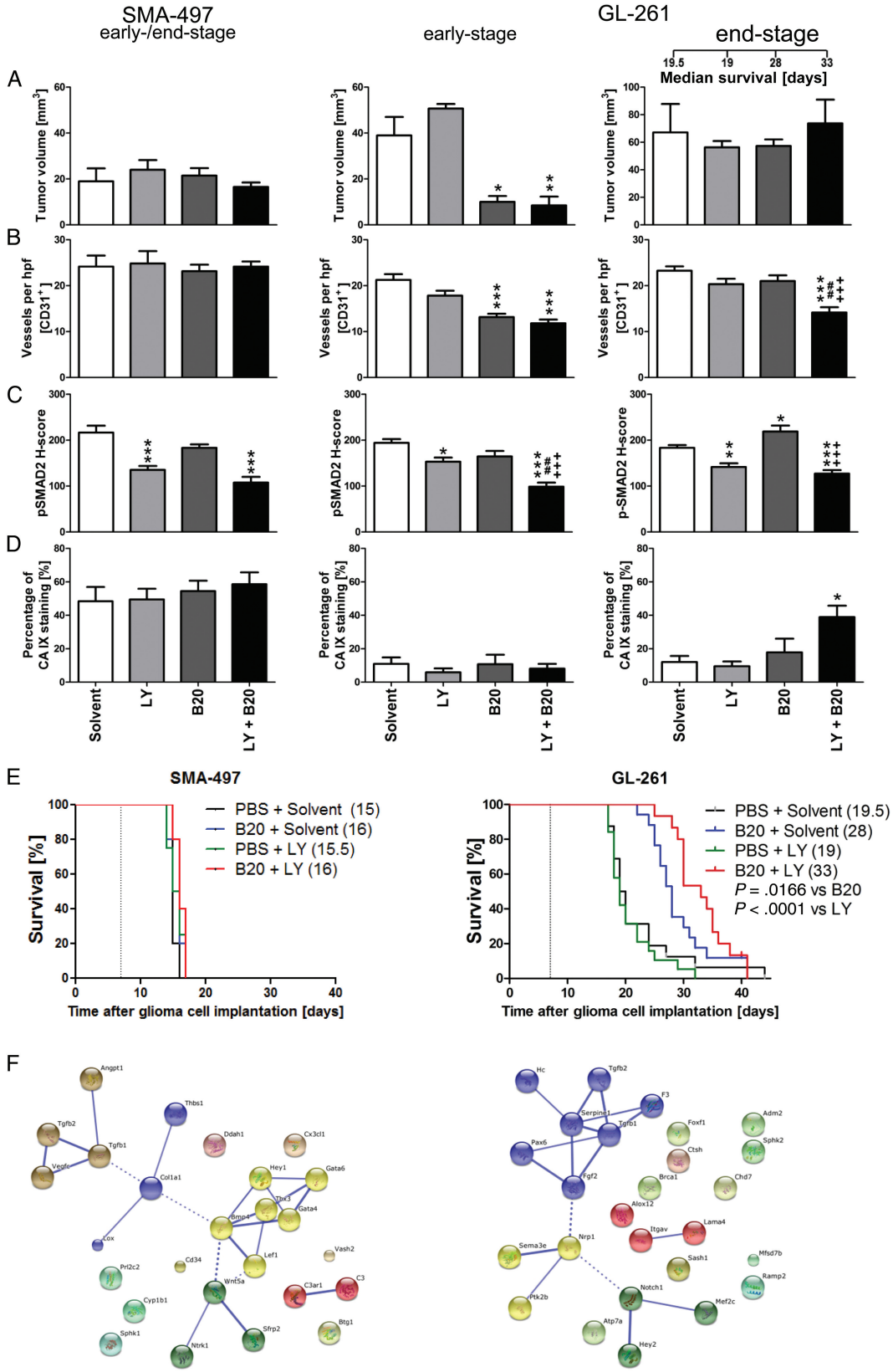

Fig. 4. Effect of combined B20 and LY2157299 treatment in SMA-497 and GL-261 syngeneic models in vivo. Syngeneic mice were intracranially implanted with SMA-497 or GL-261 cells and treated twice weekly with 5 mg/kg B20 or daily with 150 mg/kg LY2157299 or corresponding solvents

tumors possessed well-delineated margins, whereas tumor borders in the B20 treatment groups were frayed and surrounded by numerous smaller satellites in all models (Supplementary Fig. S3A and B). The number of intratumoral vessels was decreased in SMA-540, SMA-560, and GL-261, but not in SMA-497 (Fig. 2C, Supplementary Fig. S3C). Vessel morphology was specifically changed in GL-261 with decreased vessel diameter. Carbonic anhydrase (CA) 9 staining as a surrogate marker for hypoxia was strongly induced in SMA-540 and SMA-560 but still did not reach constitutive levels of the SMA-497 model (Fig. 2D, Supplementary Fig. S3D). In general, CA 9 staining was inversely related to CD31 labeling, confirming that hypoxia develops with increasing distance from blood vessels (Supplementary Fig. S3F). Finally, B20 prolonged survival in the SMA-540, SMA-560, and GL-261 models, but not in SMA-497 (Fig. 2F, Supplementary Table S1). Our hypothesis of induced activation of the TGF-β pathway as an escape route from VEGF inhibition led us to predict increased pSMAD2 levels in B20-treated tumors at least at progression. However, we observed decreased pSMAD2 levels in 2 of 4 mouse models in vivo and no change in the other 2 models; in fact, there was an association between decreased pSMAD2 levels and benefit from B20 (Fig. 2E, Supplementary Fig. S3E). This decrease in pSMAD2 levels was observed in tumor cells and tumor-infiltrating leukocytes. Tumor cells were more frequently pSMAD2 positive than host cells, indicating that tumor cells may be more responsive to TGF-β than host cells (Supplementary Fig. S3G). Further, we noted that in sharp contrast to the initial hypothesis of B20-triggered hypoxia followed by hypoxia-induced and TGF-β–mediated invasiveness, induction of hypoxia and reduction of pSMAD2 were seen in the same models. Accordingly, all 4 cell lines also responded to hypoxia with decreased pSMAD2 levels in vitro (Supplementary Fig. S2C). Bioinformatic analyses of previously published data[19] focusing on angiogenesis gene sets (Supplementary Table S2) revealed that SMA-497 expresses high levels of genes involved in angiogenic escape pathways (Fig. 2G, Supplementary Table S3). Unsupervised clustering of significantly regulated genes further revealed that genes upregulated in SMA-497 were mainly downregulated in GL-261, and vice versa (Fig. 2G, encircled clusters). Further assessment of these gene clusters by STRING analysis (Search Tool for the Retrieval of Interacting Genes/Proteins) visualized the differential activation or downregulation of genes of the angiogenic gene sets in SMA-497 and GL-261 (Supplementary Fig. S3H and I).

LY2157299 Prolongs Survival in SMA-560 and SMA-540 Murine Glioma Models

Next we determined single-agent activity of LY2157299 in the 4 mouse glioma models. Histological analyses of tumors harvested when the first clinical symptoms occurred revealed a trend toward reduced tumor volumes in only SMA-560 (Fig. 3A, Supplementary Fig. S4A). We then explored whether exposure to LY2157299 suppressed pSMAD2 as a surrogate marker of TGF-β pathway activity. Phosphorylated SMAD2 levels were decreased by LY2157299 in all models (Fig. 3B, Supplementary Fig. S4B, left), confirmed by immunoblot in SMA-560 (Supplementary Fig. S4B, right). Intratumoral vessel density was unaffected in either model, but vessel morphology was changed in all models, except SMA-497, toward a vasculature with decreased vessel diameter and lumina upon LY2157299 treatment (Fig. 3C, Supplementary Fig. S4C). LY2157299 prolonged survival in SMA-560 and SMA-540, but not SMA-497 or GL-261 (Fig. 3D, Supplementary Table S1). Accordingly, transcriptomic analysis of TGF-β receptor signaling pathway gene sets (Supplementary Table S4) showed SMA-540 and SMA-560 to be the cell lines with the highest TGF-β pathway activity (Fig. 3E, Supplementary Table S5). The survival differences in the SMA-540 control groups in the studies reported in Figs 2 and 3 are explained by variations in the tumorigenicity in this model, which is the least tumorigenic. Transcriptomic profiling also revealed that the most immunogenic tumors as defined by Gene Ontology, SMA-497 and GL-261, exhibited differential clusters of up- and downregulated genes involved in immune response pathways. Genes upregulated in SMA-497 were mainly downregulated in GL-261, and vice versa (Fig. 3F encircled, Supplementary Table S6, S7). STRING analysis of the differentially regulated gene clusters visualized the differential activation or downregulation of genes of the immune response–related gene sets in SMA-497 and GL-261 (Supplementary Fig. S4D and E).

Reciprocal Modulation of the VEGF and TGF-β Pathway In vitro

We next assessed the expression of ligands and receptors of the VEGF and TGF-β pathways in the mouse glioma models after reciprocal stimulation. First we explored whether modulation of VEGF signaling in glioma cells affected the TGF-β pathway. Exposure to exogenous VEGF, B20, or cediranib had no effect on TGF-$\beta_{1/2}$ mRNA and protein levels (Supplementary Fig. S5A and B) or pSMAD2 levels (Supplementary Fig. S5C). Conversely, VEGF mRNA expression and protein release were induced by TGF-β_2 in a LY2157299-sensitive manner. VEGF mRNA expression was also increased in all cells in response to hypoxia, whereas protein levels were increased in SMA-497, SMA-540, and GL-261 and remained similar in SMA-560 (Supplementary Fig. S5D and E). Furthermore, we observed an increase in total *VEGFR1* mRNA expression in response to TGF-β_2 in SMA-497 and SMA-560 glioma cells, which was decreased upon cotreatment with LY2157299 only in SMA-560. However, protein levels were increased in all models, and this effect was blocked by LY2157299 (Supplementary Fig. S5F).

or both from day 7 on. Brain sections from SMA-497 (early-stage) and GL-261 (early- and end-stage) were studied. (A) Tumor volumes and (B) CD31+ capillaries. (C) pSMAD2. (D) CA 9+ areas (*$P < .05$, **$P < .01$, ***$P < .001$, one-way ANOVA followed by Tukey's post hoc test 95% CI, treated vs solvent, +++$P < .001$, B20 + LY2157299 vs B20, ##$P < .01$, B20 + LY2157299 vs LY2157299). (E) Kaplan–Meier survival curves (Gehan-Breslow-Wilcoxon test, considered significant for $P < .05$). (F) Gene cluster analysis. Functional interactions between *TGFβ*$_{1/2}$ and genes upregulated in angiogenic profiles in SMA-497 (left) and GL-261 (right) were analyzed in Affymetrix microarray-based gene expression profiling by STRING analysis. Interactions with high confidence score of 0.700 were integrated into the interactome. Clusters were determined by Markov cluster algorithm and presented with different node colors. Intercluster edges are represented by dashed lines. hpf, high-powered field; PBS, phophate buffered saline.

VEGFR2 levels in response to TGF-β_2 stimulation, analyzed in SMA-540 and SMA-560 cells only, were increased upon stimulation in a LY2157299-sensitive manner (Supplementary Fig. S5G). Although LY2157299 alone reduced constitutive pSMAD2 levels (Supplementary Fig. S2B), it had no effect on constitutive VEGF ligand or receptor mRNA expression or protein release in either cell line.

Cotargeting of the VEGF and TGF-β Pathways In vivo

SMA-497 and GL-261 were chosen to explore a potential synergy between VEGF and TGF-β pathway inhibition. SMA-497 was chosen because it was refractory to either treatment as a single agent, facilitating the detection of any possible synergy. GL-261 was chosen because LY2157299 alone was not active, whereas B20 was. A gain from cotreatment would indicate that the TGF-β pathway assumes a different role in the context of VEGF inhibition. There was no survival benefit from cotreatment in SMA-497, whereas combination treatment was superior to either treatment alone in GL-261 (Fig. 4A–E, Supplementary Table S1). Early reductions of tumor volumes and blood vessel density were seen in GL-261, but not SMA-497, and only in the B20-containing regimens, with no modulation by LY2157299. The volume differences in early-stage GL-261 tumors were abolished in end-stage tumors. However, reduced blood vessel density was only maintained in the cotreatment group, but not in the B20-only end-stage tumors (Fig. 4A and B). Decreased vessel diameter and increased vessel wall thickness were observed with all therapeutic regimens in GL-261 (Supplementary Fig. S6B and F). Zonula occludens 1 was used as a marker for tight junction staining, showing a more regular staining pattern indicative for a restoration of endothelial barrier integrity (Supplementary Fig. S6I–L). Cotreatment with LY2157299 prevented B20-induced increased tumor invasiveness in early stages, but this effect was abolished in end-stage tumors (Supplementary Fig. S6A and E). In GL-261, but not SMA-497 gliomas, the reduction of pSMAD2 levels by LY2157299 alone was enhanced by cotreatment with B20 in early-stage responsive and end-stage resistant tumors. In contrast, pSMAD2 levels were increased in B20-treated end-stage tumors, consistent with the TGF-β pathway as an escape route from VEGF inhibition, and this was not seen with combined treatment (Fig. 4C, Supplementary Fig. S6C and G). There was no significant CA 9 induction in either model in early-stage tumors, whereas treatment resistance in the GL-261 cotreatment group was accompanied by an increase in CA 9 staining from 18% to 39% positive tumor areas (Fig. 4D, Supplementary Fig. S6D and H). Assessment of the role of *TGFβ*$_{1/2}$ within angiogenesis gene clusters upregulated in SMA-497 and GL-261 by STRING analysis revealed that *TGFβ*$_{1/2}$ interacts with only a small subset of upregulated genes in SMA-497. Conversely, both molecules are integrated in the main network of functional gene interactions in GL-261 (Fig. 4F), indicating a possible role of TGF-β in mediating resistance to B20 therapy.

Differential Host Cell Responses to VEGF/TGF-β Cotargeting

To generate a broad overview of host cell infiltration, we assessed frequencies of leukocytes (CD45+), T cells (CD4+ and CD8+), and macrophages/microglia (CD11b+) in mono- and cotreated SMA-497 and GL-261 early- and end-stage tumors (Fig. 5A–D, Supplementary Fig. S7A–H). In GL-261, only in early- but not in end-stage tumors, increased infiltration of CD11b+ cells upon B20 alone and increased numbers of cytotoxic T cells (CD8+) upon cotreatment were observed (Fig. 5C and D, Supplementary Fig. S7C and D). Resistance to cotreatment was accompanied by decreased infiltration of CD45+ and CD11b+ cells in GL-261 end-stage gliomas compared with solvent or B20 monotreatment (Fig. 5A and D, Supplementary Fig. S7E and H).

Phosphorylated SMAD2 was detected in tumor cells rather than host leukocytes in GL-261 end-stage tumors. Due to the higher proportion of pSMAD2+ tumor cells versus infiltrating leukocytes, tumor cells were more affected by decreased pSMAD2 levels, although levels in single leukocytes were altered similarly, with a decrease upon LY2157299 and combined treatment, and an increase by B20 alone (Fig. 6A–D).

Phosphorylated SMAD2 Levels in Response to Bevacizumab Treatment in Human Glioblastoma

We also analyzed human glioblastoma patients who underwent further surgery upon failure of bevacizumab. As groups, neither refractory tumors of 9 non-bevacizumab-treated patients nor those of 5 patients failing on a bevacizumab-containing regimen exhibited an increase or decrease in pSMAD2 levels, whereas vessel density was decreased in the latter group (Supplementary Fig. S8A–F).

Discussion

Interactions between human tumors and their specific microenvironment determine growth characteristics and responses to radiotherapy or pharmacotherapy.[20] This notion is particularly true for glioblastoma, which typically contains major host cell infiltrates which probably support rather than limit tumor growth.[21–23]

Here we focused on 2 cytokine-dependent signaling pathways attributed a major role in the pathogenesis of glioblastoma, VEGF and TGF-β, using a panel of syngeneic mouse gliomas as model systems.[19] Responsiveness to VEGF and TGF-β stimulation as assessed by VEGFR and SMAD2 phosphorylation, as well as a positive regulation of VEGF by TGF-β, but not vice versa, was confirmed in vitro (Fig. 1, Supplementary Figs S1, S2, and S5). Inhibition of neither pathway has prominent effects on glioma cell viability or growth in vitro (Supplementary Fig. S2), although growth-suppressive properties have been reported for TGF-β_1 in the SMA-560 model.[24]

There was differential responsiveness to B20-mediated VEGF inhibition alone. While high expression of VEGF and VEGFR is consistent with responsiveness of SMA-560, the responsiveness of SMA-540 was less well explained, and the expression levels of VEGF in GL-261 did not translate into superior efficacy of B20. The responsiveness of GL-261 despite unaltered proliferation and hypoxia is consistent with direct induction of cell death by VEGF inhibition in some mouse glioma models.[25,26] A high constitutive level of hypoxia and failure to reduce blood vessel density in response to B20, consistent with VEGF-independent angiogenesis, were prominent features of the refractory

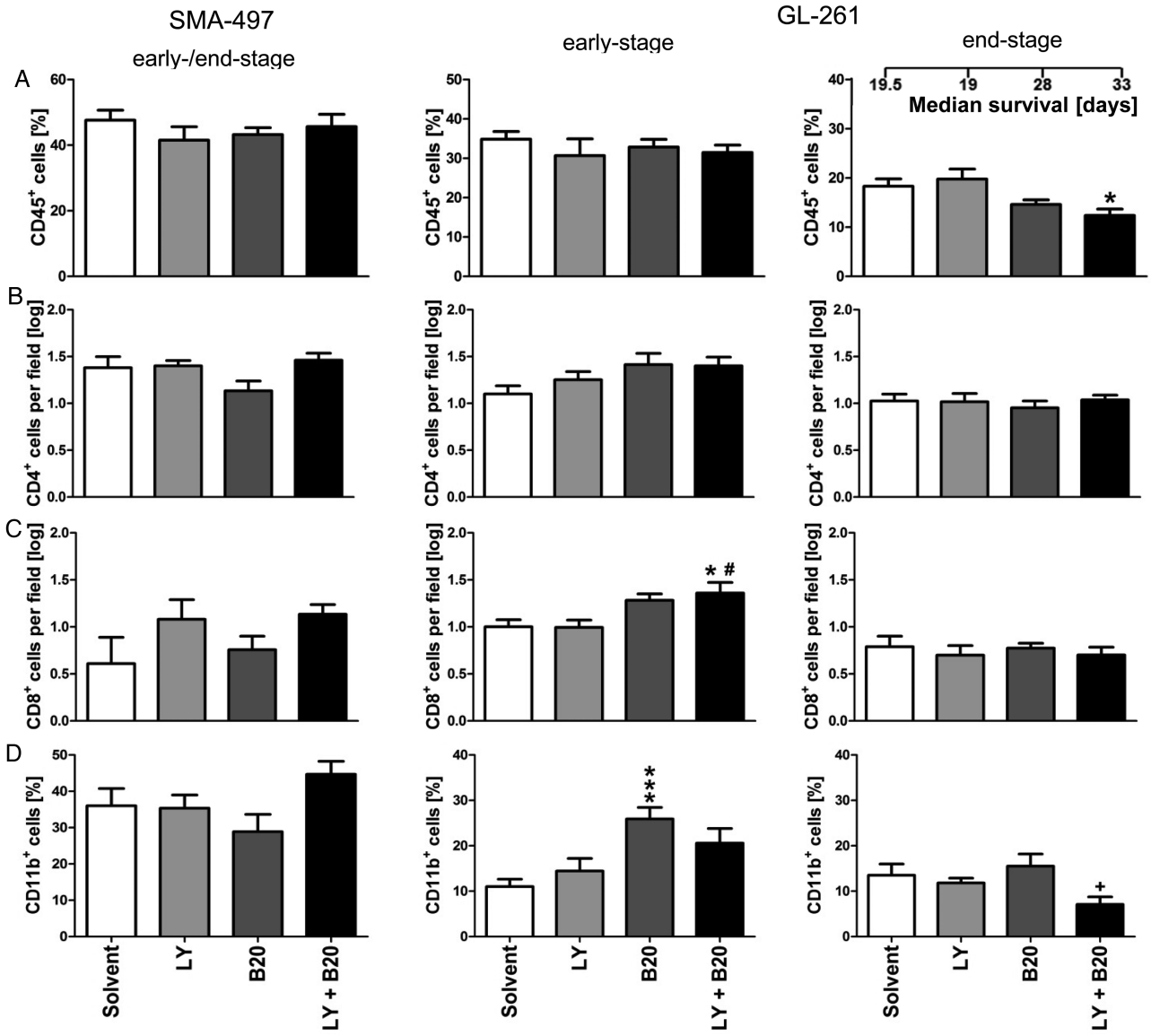

Fig. 5. Modulation of tumor immune cell infiltration in combined B20- and LY2157299-treated syngeneic models in vivo. Brain sections from SMA-497 (early-stage) and GL-261 (early- and end-stage) were examined. (A) CD45+ leukocytes. (B) CD4+ T helper cells. (C) CD8+ cytotoxic T cells. (D) CD11b+ monocytes/microglia. Data are expressed as mean + SEM (*$P < .05$ and **$P < .01$, ***$P < .001$ one-way ANOVA followed by Tukey's post hoc test 95% CI, treatment vs solvent, #$P < .05$, B20 + LY2157299 vs LY2157299, +$P < .05$, B20 + LY2157299 vs B20).

SMA-497 model. Of note, full suppression of angiogenesis was not achieved in any model (Fig. 2 and Supplementary Fig. S3). Although all SMA lines were derived from one tumor, they exhibited major variation in response to different treatment settings that were tentatively linked to differential transcriptomics specifically among angiogenesis-related gene sets (Fig. 2, Supplementary Tables S2, S3).

The TGF-βR1 inhibitor LY2157299 was active pharmacodynamically as assessed by a decrease of pSMAD2 levels in vivo, although no full suppression was achieved, indicating either insufficient pharmacodynamic properties and target coverage or ALK-5–independent pathways maintaining pSMAD2 phosphorylation, or both (Fig. 3 and Supplementary Table S4). The 2 models responsive to LY2157299 in vivo, SMA-540 and SMA-560, exhibited increased expression levels of genes of the TGF-β receptor signaling pathway (Fig. 3). Similar to anti-angiogenic therapy, TGF-β antagonism has been linked to vascular normalization and improved drug delivery.[27] Accordingly, we observed morphological changes related to vascular normalization in tumor vessels upon LY2157299 treatment in all models, consisting of increased vessel wall thickness and decreased vessel diameter (Fig. 3C, Supplementary Fig. S4C). It is tempting to link these uniform changes in blood vessel morphology, induced by LY2157299, to the effects of TGF-β on VEGF and VEGFR expression in vitro (Supplementary Figs S4, S5). A transcriptional profiling study of human glioblastoma

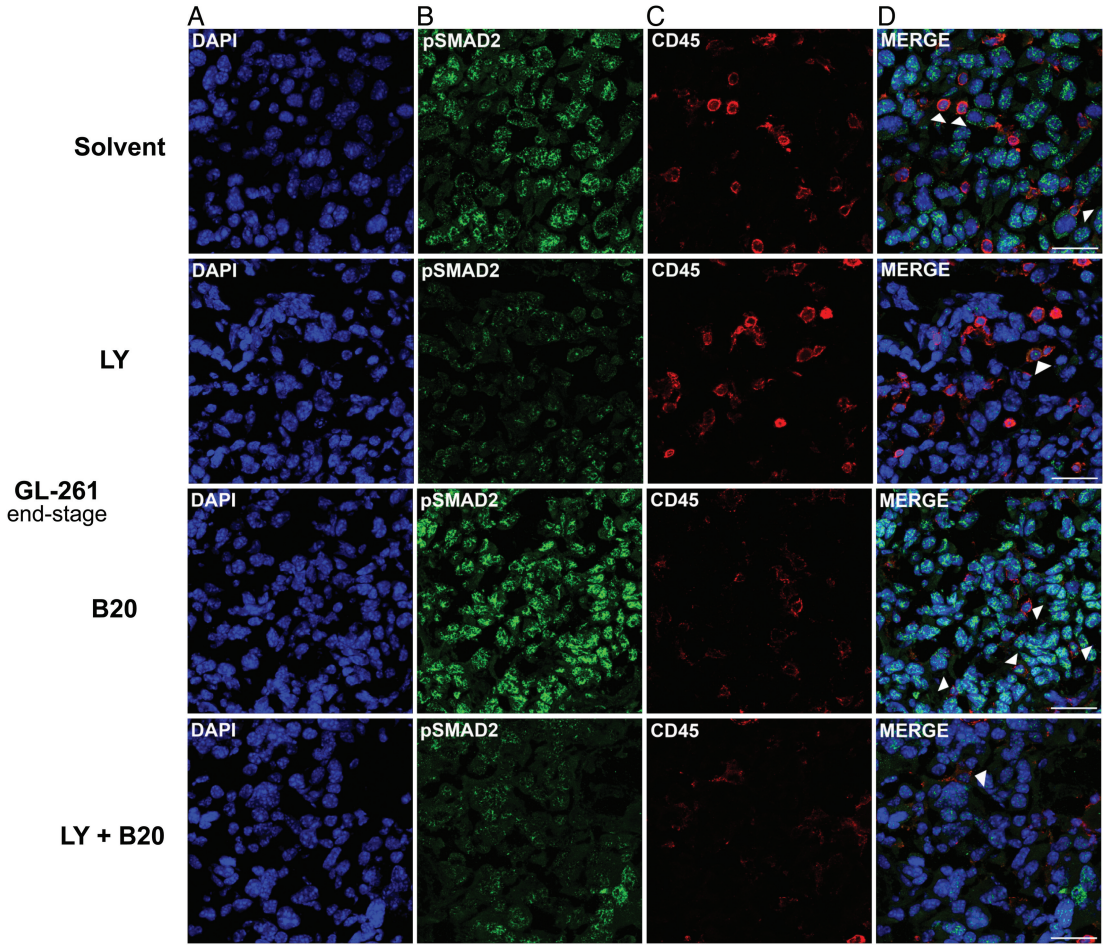

Fig. 6. Modulation of pSMAD2 levels and tumor immune cell infiltration in B20 and LY2157299 cotreated GL-261 syngeneic model in vivo. Brain sections (end-stage) were examined. Staining of tumor sections was assessed with (A) 4′,6′-diamidino-2-phenylindole (DAPI) (blue), (B) pSMAD2 (green), and (C) CD45 (red). Merged images are shown in (D). CD45+/pSMAD2+ leukocytes are marked by arrowheads. Scale bars correspond to 50 μm.

vessels indicated key roles in the process of pathological angiogenesis for VEGFA and TGFβ2.[28] The decrease in pSMAD2 levels in response to hypoxia in vitro and to hypoxia in association with B20 treatment in vivo in 2 of 3 responsive models was surprising (Fig. 2, Supplementary Fig. S2), since no evidence suggests that the TGF-β pathway is negatively regulated by hypoxia. Interestingly, pSMAD2 levels positively correlated with tumor proliferation in human glioblastoma.[9] Accordingly, we also found parallel changes in the levels of both markers (Fig. 2, Supplementary Fig. S2).

VEGFR inhibition in vitro did not decrease pSMAD2 levels in any cell line (Supplementary Fig. S5). Yet, the synergistic suppression of pSMAD2 levels by B20 and LY2157299 cotreatment in early-stage tumors and increased pSMAD2 levels in end-stage tumors with B20 treatment alone are consistent with the hypothesis that enhanced TGF-β activity might promote eventual escape from VEGF inhibition at least in the GL-261 model. Immunohistochemical analysis of orthotopic U87MG gliomas had indeed revealed increased TGF-β protein levels upon anti-VEGF treatment.[29]

Increased levels of CD11b+ macrophages/microglia have been linked to refractoriness to anti-VEGF treatment[30] and have been attributed a role in the VEGF-independent restoration of tumor vessels by vasculogenic but not angiogenic processes.[31] Supporting this concept, we observed that cotargeting VEGF and TGF-βR1 decreased the numbers of intratumoral CD11b+ cells and that tumors failed to revascularize compared with B20 alone in GL-261 end-stage tumors (Fig. 5 and Supplementary Figs S6, S7). Similarly, coinhibition of VEGF and the angiopoietin-2 pathway provided improved tumor control and reduced numbers of F4/80+ macrophages in the GL-261 model.[25] Possibly, targeting TGF-β alters CD11b+ cell recruitment via interacting with the chemokine (C-X-C motif) receptor 4 (CXCR4)–CXCL12 axis, since VEGFR inhibitors can upregulate CXCR4 in glioblastoma cells by a TGF-β–dependent mechanism[32] and TGF-β upregulates CXCR4 expression in monocytes, macrophages, naïve T cells, and other immune cell populations.[33,34]

Altogether, according to our analysis in the GL-261 model, the tumor-promoting role of TGF-β would relate more to facilitating angiogenesis or vasculogenesis than to promoting a more invasive phenotype even when combined with VEGF antagonists. This is because B20-treated tumors were more invasive early on when pSMAD2 levels were still low and because

cotreatment with LY2157299 still suppressed tumor vasculature in end-stage disease (Figs 2 and 4). Yet, B20-induced hypoxia may ultimately promote lactate dehydrogenase activity,[35] which in turn may stimulate TGF-β signaling associated with an angiogenic signaling.[36]

Unexpectedly, we observed that mainly tumor cells but not leukocytes exhibited pSMAD2 (Fig. 6 and Supplementary Fig. S3). Previous studies have already indicated that pSMAD2 levels are high in glioblastoma cells, indicating that tumor cells do not have to escape TGF-β signaling at least at the level of SMAD2 phosphorylation.[9,37] However, pSMAD2 levels in B20-treated GL-261 end-stage tumors increased proportionally in tumor cells and leukocytes (Fig. 6). Since the activation of TGF-β signaling in tumors has been linked to immunosuppression,[38] increased pSMAD2 levels indicate a TGF-β–induced immunosuppressive tumor micromilieu during anti-VEGF treatment, which might be an important factor of therapy failure. Yet, preliminary studies in paired human glioblastoma samples provided no evidence for enhanced pSMAD2 levels at recurrence, either without or with previous bevacizumab therapy (Supplementary Fig. S8).

Limitations of the present study include the challenges in determining volumes of infiltrative rodent gliomas, the restriction to mouse models based on long-term cell lines, and the exploration of cotreatment rather than sequential treatments. Moreover, we did not distinguish B20 or LY2157299 effects on tumor versus host cells and effects of B20 on VEGFR1 versus VEGFR2 signaling in mouse glioma cells,[39] and the human patient cohort was small.

Our study highlights the relevance of hypoxia in the malignant phenotype of glioblastoma and its resistance to therapy. SMA-497 showed the highest constitutive level of hypoxia and was refractory to all therapeutic interventions. GL-261 eventually became hypoxic when escaping combination therapy (Fig. 4 and Supplementary Fig. S6). We conclude that at least for subsets of glioblastomas, cotargeting of VEGF and TGF-β pathways might result in a permanent vascularization deficiency, which results in prolonged tumor control. Ultimately, however, such microenvironment-targeting therapies may only be successful if combined with pharmacological or cell-based therapies that exert relevant tumor cell cytotoxicity, since the major cell biological changes observed in selected models did not translate into major gains in survival.

Supplementary material

Supplementary material is available at *Neuro-Oncology Journal* online (http://neuro-oncology.oxfordjournals.org/).

Funding

This study was supported by a grant from Oncosuisse (KFS-02694-08-2010) to M.W. and G.T.

Acknowledgments

We thank Michael Lahn (Eli Lilly & Co) for valuable discussions.

Conflict of interest statement. M.W. has received research grants from Roche and honoraria for lectures or advisory board participation from Lilly and Roche. K.S. has received honoraria from Roche for advisory board participation. G.R. has received research grants from Roche and Merck as well as honoraria for lectures or advisory board participation from Amgen and Celldex. G.T. received research and travel grants and honoraria for lectures and advisory board participation from Roche. The authors declare no additional competing financial interests.

References

1. Weller M, van den Bent M, Hopkins K, et al. EANO guideline for the diagnosis and treatment of anaplastic gliomas and glioblastoma. *Lancet Oncol*. 2014;15(9):e395–e403.
2. Weller M, Wick W, Aldape K, et al. Glioma. *Nat Rev Dis Primers*. 2015:15017.
3. Wick W, Brandes A, Gorlia T, et al. LB-05 phase III trial exploring the combination of bevacizumab and lomustine in patients with first recurrence of a glioblastoma: the EORTC 26101 trial. *Neuro Oncol*. 2015;17(suppl 5):v1.
4. Chinot OL, Wick W, Mason W, et al. Bevacizumab plus radiotherapy-temozolomide for newly diagnosed glioblastoma. *N Engl J Med*. 2014;370(8):709–722.
5. Gilbert MR, Dignam JJ, Armstrong TS, et al. A randomized trial of bevacizumab for newly diagnosed glioblastoma. *N Engl J Med*. 2014;370(8):699–708.
6. Paez-Ribes M, Allen E, Hudock J, et al. Antiangiogenic therapy elicits malignant progression of tumors to increased local invasion and distant metastasis. *Cancer cell*. 2009;15(3):220–231.
7. Wick A, Dorner N, Schafer N, et al. Bevacizumab does not increase the risk of remote relapse in malignant glioma. *Ann Neurol*. 2011;69(3):586–592.
8. Wick W, Cloughesy TF, Nishikawa R, et al. Tumor response based on adapted Macdonald criteria and assessment of pseudoprogression (PsPD) in the phase III AVAglio trial of bevacizumab (Bv) plus temozolomide (T) plus radiotherapy (RT) in newly diagnosed glioblastoma (GBM). *J Clin Oncol*. 2013;31(15).
9. Bruna A, Darken RS, Rojo F, et al. High TGFbeta-Smad activity confers poor prognosis in glioma patients and promotes cell proliferation depending on the methylation of the PDGF-B gene. *Cancer cell*. 2007;11(2):147–160.
10. Rodon J, Carducci MA, Sepulveda-Sanchez JM, et al. First-in-human dose study of the novel transforming growth factor-beta receptor I kinase inhibitor LY2157299 monohydrate in patients with advanced cancer and glioma. *Clin Cancer Res*. 2015;21(3):553–560.
11. Herbertz S, Sawyer JS, Stauber AJ, et al. Clinical development of galunisertib (LY2157299 monohydrate), a small molecule inhibitor of transforming growth factor-beta signaling pathway. *Drug Des Devel Ther*. 2015;9:4479–4499.
12. Hjelmeland MD, Hjelmeland AB, Sathornsumetee S, et al. SB-431542, a small molecule transforming growth factor-beta-receptor antagonist, inhibits human glioma cell line proliferation and motility. *Mol Cancer Ther*. 2004;3(6):737–745.
13. Seystahl K, Tritschler I, Szabo E, et al. Differential regulation of TGF-beta-induced, ALK-5-mediated VEGF release by SMAD2/3 versus SMAD1/5/8 signaling in glioblastoma. *Neuro Oncol*. 2015;17(2):254–265.
14. Pertovaara L, Kaipainen A, Mustonen T, et al. Vascular endothelial growth factor is induced in response to transforming growth factor-beta in fibroblastic and epithelial cells. *J Biol Chem*. 1994;269(9):6271–6274.

15. Pepper MS, Vassalli JD, Orci L, et al. Biphasic effect of transforming growth factor-beta 1 on in vitro angiogenesis. *Exp Cell Res*. 1993; 204(2):356–363.
16. Pepper MS. Transforming growth factor-beta: vasculogenesis, angiogenesis, and vessel wall integrity. *Cytokine Growth Factor Rev*. 1997;8(1):21–43.
17. Happold C, Roth P, Silginer M, et al. Interferon-beta induces loss of spherogenicity and overcomes therapy resistance of glioblastoma stem cells. *Mol Cancer Ther*. 2014;13(4):948–961.
18. Roth P, Silginer M, Goodman SL, et al. Integrin control of the transforming growth factor-beta pathway in glioblastoma. *Brain*. 2013;136(Pt 2):564–576.
19. Ahmad M, Frei K, Willscher E, et al. How stemlike are sphere cultures from long-term cancer cell lines? Lessons from mouse glioma models. *J Neuropathol Exp Neurol*. 2014;73(11): 1062–1077.
20. Hanahan D, Weinberg RA. Hallmarks of cancer: the next generation. *Cell*. 2011;144(5):646–674.
21. Murdoch C, Muthana M, Coffelt SB, et al. The role of myeloid cells in the promotion of tumour angiogenesis. *Nat Rev Cancer*. 2008;8(8): 618–631.
22. Maes W, Verschuere T, Van Hoylandt A, et al. Depletion of regulatory T cells in a mouse experimental glioma model through anti-CD25 treatment results in the infiltration of non-immunosuppressive myeloid cells in the brain. *Clin Dev Immunol*. 2013;2013:952469.
23. Vom Berg J, Vrohlings M, Haller S, et al. Intratumoral IL-12 combined with CTLA-4 blockade elicits T cell-mediated glioma rejection. *J Exp Med*. 2013;210(13):2803–2811.
24. Ashley DM, Sampson JH, Archer GE, et al. Local production of TGF beta1 inhibits cerebral edema, enhances TNF-alpha induced apoptosis and improves survival in a murine glioma model. *J Neuroimmunol*. 1998;86(1):46–52.
25. Scholz A, Harter PN, Cremer S, et al. Endothelial cell-derived angiopoietin-2 is a therapeutic target in treatment-naive and bevacizumab-resistant glioblastoma. *EMBO Mol Med*. 2015;8(1): 39–57.
26. Pitter KL, Tamagno I, Alikhanyan K, et al. Corticosteroids compromise survival in glioblastoma. *Brain*. 2016;139(Pt5): 1458–1471.
27. Liu J, Liao S, Diop-Frimpong B, et al. TGF-beta blockade improves the distribution and efficacy of therapeutics in breast carcinoma by normalizing the tumor stroma. *Proc Natl Acad Sci USA*. 2012; 109(41):16618–16623.
28. Dieterich LC, Mellberg S, Langenkamp E, et al. Transcriptional profiling of human glioblastoma vessels indicates a key role of VEGF-A and TGFbeta2 in vascular abnormalization. *J Pathol*. 2012;228(3):378–390.
29. Piao Y, Liang J, Holmes L, et al. Glioblastoma resistance to anti-VEGF therapy is associated with myeloid cell infiltration, stem cell accumulation, and a mesenchymal phenotype. *Neuro Oncol*. 2012;14(11):1379–1392.
30. Shojaei F, Wu X, Malik AK, et al. Tumor refractoriness to anti-VEGF treatment is mediated by CD11b + Gr1+ myeloid cells. *Nat Biotechnol*. 2007;25(8):911–920.
31. Kioi M, Vogel H, Schultz G, et al. Inhibition of vasculogenesis, but not angiogenesis, prevents the recurrence of glioblastoma after irradiation in mice. *J Clin Invest*. 2010;120(3):694–705.
32. Pham K, Luo D, Siemann DW, et al. VEGFR inhibitors upregulate CXCR4 in VEGF receptor-expressing glioblastoma in a TGFbetaR signaling-dependent manner. *Cancer Lett*. 2015;360(1):60–67.
33. Wang J, Guan E, Roderiquez G, et al. Role of tyrosine phosphorylation in ligand-independent sequestration of CXCR4 in human primary monocytes-macrophages. *J Biol Chem*. 2001; 276(52):49236–49243.
34. Franitza S, Kollet O, Brill A, et al. TGF-beta1 enhances SDF-1alpha-induced chemotaxis and homing of naive T cells by up-regulating CXCR4 expression and downstream cytoskeletal effector molecules. *Eur J Immunol*. 2002;32(1):193–202.
35. Fack F, Espedal H, Keunen O, et al. Bevacizumab treatment induces metabolic adaptation toward anaerobic metabolism in glioblastomas. *Acta Neuropathol*. 2015;129(1):115–131.
36. Baumann F, Leukel P, Doerfelt A, et al. Lactate promotes glioma migration by TGF-beta2-dependent regulation of matrix metalloproteinase-2. *Neuro Oncol*. 2009;11(4):368–380.
37. Frei K, Gramatzki D, Tritschler I, et al. Transforming growth factor-beta pathway activity in glioblastoma. *Oncotarget*. 2015; 6(8):5963–5977.
38. Rich JN. The role of transforming growth factor-beta in primary brain tumors. *Front Biosci*. 2003;8:e245–e260.
39. Szabo E, Schneider H, Seystahl K, et al. Autocrine VEGFR1 and VEGFR2 signaling promotes survival in human glioblastoma models in vitro and in vivo. *Neuro Oncol*. 2016; in press.